

Dynamic nonlinear hysteretic effective stress analysis in geotechnical engineering

W.D.Liam Finn & M.Yogendrakumar
University of British Columbia, Vancouver, Canada
N.Yoshida
Sato Kogyo Ltd, Tokyo, Japan

ABSTRACT: A method for dynamic nonlinear, hysteretic, effective stress analysis is presented which is applicable to embankment dams and soil-structure systems. The method is validated by data from a simulated earthquake test on a centrifuged model of a structure embedded in a saturated sand foundation. The utility of the analysis in engineering practice is demonstrated by the dynamic response analysis of a tailings dam on a nonhomogeneous foundation.

1. INTRODUCTION

The basic elements in the dynamic analysis of a soil-structure system are input motion, appropriate models of site and structure, constitutive relations for all materials present, and a stable, efficient, accurate, computational procedure.

Linear elastic analysis is appropriate for low levels of shaking in relatively firm ground. As the shaking becomes more intense, soil response becomes nonlinear. A great variety of constitutive relations are available for nonlinear response analysis ranging from equivalent linear elastic models to elastic-plastic models with both isotropic and kinematic hardening.

The most widely used methods for dynamic analysis are based on the equivalent linear model. Computer programs representative of this approach are SHAKE (Schnabel et al., 1972) for one-dimensional analysis (1-D) and FLUSH (Lysmer et al., 1975) for 2-D analysis. These programs perform total stress analyses only. Equivalent linear models can exhibit pseudo-resonance, an amplification of computed response that is a function of the nature of the model only. This phenomenon can lead to increased design requirements (Finn et al., 1978).

The dynamic response characteristics and stability of an earth structure during earthquakes are controlled by the effective stress regime in the structure. In saturated regions of the structure,

porewater pressures are induced by seismic excitation. These pressures continuously modify the effective stresses during the earthquake and hence have a major impact on dynamic response and stability; in extreme cases, they can trigger flow slides.

It is clearly a very important step in the design process to make reliable estimates of seismically induced porewater pressures. A semi-empirical method of estimation was developed by Seed (1979a), which is widely used in practice. Since 1976, there has been growing interest in the development and application of effective stress methods of dynamic response analysis (Finn et al., 1976, 1986; Dikmen and Ghabbousi, 1984; Ishihara and Towhata, 1982; Prevost et al., 1981; Siddharthan and Finn, 1982; and Zienkiewicz et al., 1978). These methods model the important phenomenological aspects of dynamic response of saturated soils. However, because of a lack of data from suitably instrumented structures in the field it has not been possible to validate the quantitative predictive capabilities of the methods except in a few cases of level ground conditions (Finn et al., 1982; Iai et al., 1985).

A limited validation of these methods has been possible using data from element tests such as cyclic triaxial or simple shear tests (Finn and Bhatia, 1980). Although this type of validation is an important first step, it is inadequate

because in these tests either the stress or strain field is prescribed and both are considered homogeneous. Therefore, the tests do not provide the rigorous trial of either the constitutive relations or the robustness of the computational procedure that data from an instrumented structure in the field with inhomogeneous stress and strain fields would make possible.

There are two procedures for modelling the complex response of field structures, a model test conducted on a shake table or in a centrifuge. In a centrifuged model, stresses at the same levels that exist in a full scale structure at corresponding points can be produced by creating an artificial gravity field of intensity Ng , where g is the acceleration due to the gravity of the earth and $1/N$ is the linear scale of the model. This ability to create prototype stresses in the model is important since soil properties are dependent on effective stresses. For this reason, seismic tests on a centrifuged model are considered superior to those conducted on a shaking table in a lg environment. Since the static stress levels in both model and prototype are similar at corresponding points, each soil element in the centrifuged model may be expected to undergo the same response history as corresponding elements in the prototype for a given excitation (Barton, 1982).

The United States Nuclear Regulatory Commission (USNRC) through the U.S. Army Corps of Engineers sponsored a series of centrifuged model tests to provide data for the verification of the dynamic nonlinear effective stress method of analysis incorporated in the program TARA-3 (Finn et al., 1986). The tests were conducted on the large geotechnical centrifuge at Cambridge University in the United Kingdom. Details of the Cambridge centrifuge and associated procedures for simulated earthquake testing have been described by Schofield (1981). Some of the USNRC tests will be described and analyzed to demonstrate current capability in dynamic effective stress analysis and seismic porewater pressure estimation. Analyses of other tests may be found in Finn (1985) and Finn et al. (1984, 1985a, 1985b).

2. METHOD OF ANALYSIS BY TARA-3

An incrementally elastic approach has been adopted to model nonlinear behaviour

using tangent shear and bulk moduli, G_t and B_t respectively. The incremental dynamic equilibrium forces $\{\Delta P\}$ are given by

$$[M]\{\Delta \ddot{x}\} + [C]\{\Delta \dot{x}\} + [K]\{\Delta x\} = \{\Delta P\} \quad (1)$$

where $[M]$, $[C]$ and $[K]$ are the mass, damping and stiffness matrices respectively, and $\{\Delta x\}$, $\{\Delta \dot{x}\}$, $\{\Delta \ddot{x}\}$ are the matrices of incremental relative displacements, velocities and accelerations. The viscous damping is of the Rayleigh type and the stiffness matrix is a function of the current tangent moduli. The use of shear and bulk moduli allows the elasticity matrix $[D]$ to be expressed as

$$[D] = B_t [Q_1] + G_t [Q_2] \quad (2)$$

where $[Q_1]$ and $[Q_2]$ are constant matrices for the plane strain conditions usually considered in analyses. This formulation reduces the computation time for formulating $[D]$ whenever G_t and B_t change in magnitude because of straining or porewater pressure changes.

2.1 Stress-Strain Behaviour

The behaviour of soil in shear is assumed to be nonlinear and hysteretic, exhibiting Masing behaviour (1926) during unloading and reloading. Therefore damping is primarily hysteretic.

The response of the soil to uniform all round pressure is assumed to be nonlinearly elastic and dependent on the mean normal stress. In this deformation mode, hysteresis is neglected.

The relationship between shear stress τ and shear strain γ for the initial loading phase under either drained or undrained loading conditions is assumed to be hyperbolic and given by

$$\tau = f(\gamma) = \frac{G_{\max} \gamma}{(1 + (G_{\max}/\tau_{\max}) |\gamma|)} \quad (3)$$

in which G_{\max} = maximum shear modulus and τ_{\max} = appropriate shear strength. This initial loading or skeleton curve is shown in Fig. 1(a). The unloading-reloading has been modelled using the Masing criterion. This implies that the equation for the unloading curve from a point (γ_r, τ_r) at which the loading reverses direction is given by

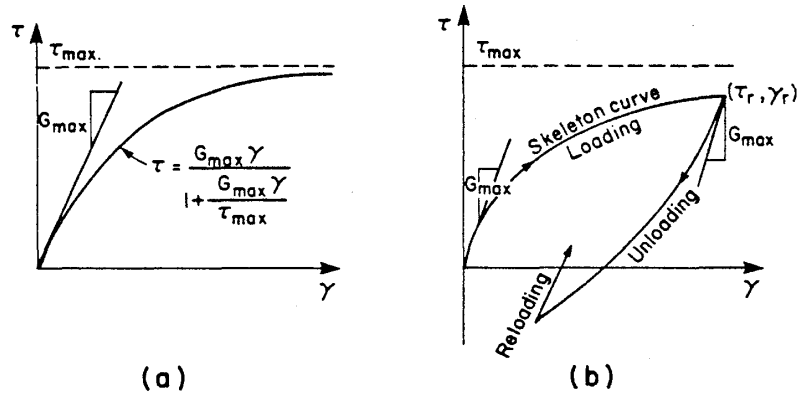


Figure 1. (a) Initial loading curve; (b) Masing stress strain curves for unloading and reloading.

$$\frac{\tau - \tau_r}{2} = \frac{G_{\max}(\gamma - \gamma_r)/2}{1 + (G_{\max}/2\tau_{\max})|\gamma - \gamma_r|} \quad (4)$$

or

$$\frac{\tau - \tau_r}{2} = f\left(\frac{\gamma - \gamma_r}{2}\right) \quad (5)$$

The shape of the unloading-reloading curve is shown in Fig. 1(b).

Finn et al. (1976) proposed rules for extending the Masing concept to irregular loading. They suggested that unloading and reloading curves follow the skeleton loading curve when the magnitude of the previous maximum shear strain is exceeded.

The stiffness matrix [K] in Eqn. 1 is determined using the appropriate tangent shear modulus, G_t , derived from Eqn. 4 and the bulk modulus, B_t from

$$B_t = K_b P_a \left(\frac{\sigma_m}{P_a}\right)^n \quad (6)$$

in which K_b is the bulk modulus constant, P_a is atmospheric pressure, σ_m is the current mean normal effective stress and n is a constant for a given soil type. K_b and n are determined by triaxial tests (Duncan and Chang, 1970).

Both G_t and B_t depend on the current mean-normal effective stress $\sigma_m' = \sigma_m - u$, in which σ_m is the total mean normal stress and u the current seismically induced porewater pressure. Therefore, as the porewater pressure increases and reduces the mean effective stresses, these parameters must be adjusted accordingly. For

example, it is commonly assumed that $G_{\max} \propto (\sigma_m')^{1/2}$, therefore

$$\frac{G}{G_{\max}} = \left(\frac{\sigma_m'}{\sigma_{m0}'}\right)^{1/2} \quad (7)$$

where G = maximum shear modulus for the current cycle of loading (Finn et al., 1976).

If significant volumetric compaction occurs during seismic loading, the moduli should also be modified to reflect this strain hardening, following procedures outlined by Finn et al. (1976). The program continuously modifies the soil properties for the effects of porewater pressures and dynamic strains.

2.2 Residual Porewater Pressure Model

During seismic shaking two kinds of porewater pressures are generated in saturated sands; transient and residual. The transient pressures are due to changes in the applied mean normal stresses during seismic excitation. For saturated sands, the transient changes in porewater pressures are equal to changes in the mean normal stresses. Since they balance each other, the effective stress regime in the sand remains largely unchanged and so the stability and deformability of the sand is not seriously affected.

The residual porewater pressures are due to plastic deformations in the sand skeleton. These persist until dissipated by drainage or diffusion and therefore they exert a major influence on the strength and stiffness of the sand skeleton. Since the shear and bulk moduli are

dependent on the effective stresses in the soil, excess porewater pressures must be continually updated during analysis, and their effects on the moduli taken progressively into account. Two porewater pressure models are available; the Martin-Finn-Seed model (Martin et al., 1975) and the Finn-Bhatia (1981) endochronic model. The M-F-S model was used in the subsequent analyses to generate the residual porewater pressures. Therefore computed porewater pressure records will show the steady accumulation of pressure with time but will not show the fluctuations in pressure caused by the transient changes in mean normal stresses.

In the Martin-Finn-Seed model the increments in porewater pressure ΔU that develop in a saturated sand under seismic shear strains are related to the volumetric strain increments $\Delta \epsilon_{vd}$ that occur in the same sand under drained conditions with the same shear strain history. The original model applies only to level ground, so that there are no static shear stresses acting on horizontal planes prior to the earthquake. The M-F-S model was subsequently modified to include the effects of the initial static shear stresses present in 2-D analyses as described later.

The porewater pressure model is described by

$$\Delta U = \bar{E}_r \cdot \Delta \epsilon_{vd} \quad (8)$$

in which \bar{E}_r = one-dimensional rebound modulus of sand at an effective stress σ'_v .

Under drained simple shear conditions, the volumetric strain increment $\Delta \epsilon_{vd}$ is a function of the total accumulated volumetric strain ϵ_{vd} and the amplitude of the current shear strain γ , and is given by

$$\Delta \epsilon_{vd} = C_1(\gamma - C_2 \epsilon_{vd}) + \frac{C_3 \epsilon_{vd}^2}{\gamma + C_4 \epsilon_{vd}} \quad (9)$$

in which C_1 , C_2 , C_3 and C_4 are volume change constants that depend on the sand type and relative density and may be determined experimentally by means of drained cyclic simple shear tests on dry or saturated samples.

An analytical expression for the rebound modulus \bar{E}_r , at any effective stress level σ'_v , is given by Martin et al. (1975) as

$$\bar{E}_r = \frac{d\sigma'_v}{d\epsilon_{vr}} = (\sigma'_v)^{1-m} / [m K_2 (\sigma'_{v0})^{n-m}] \quad (10)$$

in which σ'_{v0} is the initial value of the effective stress and K_2 , m and n are experimental constants derived from rebound tests in a consolidation ring.

2.3 Determination of Porewater Pressure Constants in Practice

The direct measurement of the constants in the porewater pressure model requires cyclic simple shear equipment which is not yet in common use. Therefore, to facilitate the use of TARA-3 in practice, techniques have been developed to derive the constants from the liquefaction resistance curve of the soil. The liquefaction curve may be determined from cyclic triaxial tests and then corrected to simple shear conditions as described by Seed (1979b) or derived directly from Standard Penetration Test data (Seed et al., 1983). In the latter case the constants are derived by a regression process to ensure that the predicted liquefaction curve compares satisfactorily with the field liquefaction curve using the program SIMCYC2 (Yogendrakumar and Finn, 1986a). If the liquefaction curve has been derived by laboratory tests, the rate of porewater pressure increase is known. Then a program for regression analysis, C-PRO, (Yogendrakumar and Finn, 1986b) is used to select constants that match both the rate of porewater pressure generation and the liquefaction curve.

This process has been adapted to the TARA-3 model to include the effects of static shear. The volumetric strain constants are derived from porewater pressure data from cyclic loading tests with various levels of static shear stress or from appropriate liquefaction resistance curves reflecting the influence of initial static shear.

2.4 Slip Elements

For analysis involving soil-structure interaction it may be important to model slippage between the structure and soil. Slip may occur during very strong shaking or even under moderate shaking if high porewater pressures are developed under the structure. TARA-3 contains slip

elements of the type developed by Goodman et al., (1968), to allow for relative movement between soil and structure in both sliding and rocking modes during earthquake excitation.

3. RESPONSE OF SATURATED EMBANKMENT WITH EMBEDDED STRUCTURE

A schematic view of a saturated embankment with an embedded structure is shown in Fig. 2. This configuration with a strong soil-structure interaction provides a very severe test of the capabilities of TARA-3 to model dynamic response. The structure is made from a solid piece of aluminum alloy and has dimensions 150mm wide by 108mm high in the plane of shaking. The length perpendicular to the plane of shaking is 470mm and spans the width of the model container. The structure is embedded a depth of 25mm in the sand foundation. Sand was glued to the base of the structure to prevent slip between structure and sand.

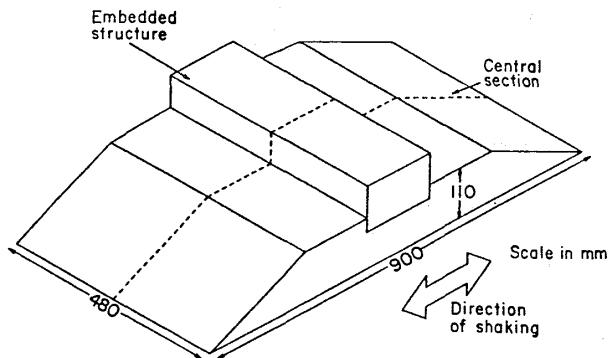


Figure 2. Centrifugal model of embedded structure.

The foundation was constructed of Leighton Buzzard Sand passing BSS No. 52 and retained on BSS No. 100. The mean grain size is therefore 0.225mm. The sand was placed as uniformly as possible to a nominal relative density $D_r = 52\%$.

During the test the model experienced a nominal centrifugal acceleration of 80 g. The model therefore simulated a structure approximately 8.6m high by 12m wide embedded 2m in the foundation sand.

De-aired silicon oil with a viscosity of 80 centistokes was used as a pore fluid. In the gravitational field of

80g, the structure underwent consolidation settlement which led to a significant increase in density under the structure compared to that in the free field. This change in density was taken into account in the analysis.

The locations of the accelerometers (ACC) and pressure transducers (PPT) are shown in Fig. 3. Analyses of previous centrifuge tests indicated that TARA-3 was capable of modelling acceleration response satisfactorily. Therefore, in the present test, more instrumentation was devoted to obtaining a good data base for checking the ability of TARA-3 to predict residual porewater pressures.

As may be seen in Fig. 3, the porewater pressure transducers are duplicated at corresponding locations on both sides of the centre line of the model except for PPT 2255 and PPT 1111. The purpose of this duplication was to remove any uncertainty as to whether a difference between computed and measured porewater pressures might be due simply to local inhomogeneity in density.

The porewater pressure data from all transducers are shown in Fig. 4. These records show the sum of the transient and residual porewater pressures. The peak residual pressure may be observed when the excitation has ceased at about 95 milliseconds. The pressures recorded at corresponding points on opposite sides of the centre line such as PPT 2631 and PPT 2338 are generally quite similar although there are obviously minor differences in the levels of both total and residual porewater pressures. Therefore it can be assumed that the sand foundation is remarkably symmetrical in its properties about the centre line of the model.

3.1 Computed and Measured Acceleration Responses

The soil-structure interaction model was converted to prototype scale before analysis using TARA-3 and all data are quoted at prototype scale. Soil properties were consistent with relative density.

The computed and measured horizontal accelerations at the top of the structure at the location of ACC 1938 are shown in Fig. 5. They are very similar in frequency content, each corresponding to the frequency of the input motion given by ACC 3441 (Fig. 4). The peak accelerations agree fairly closely.

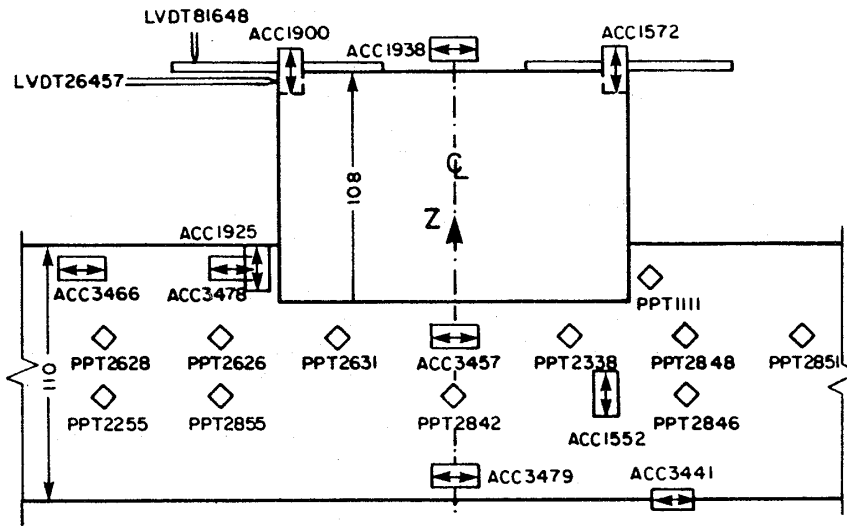


Figure 3. Instrumentation of centrifuged model.

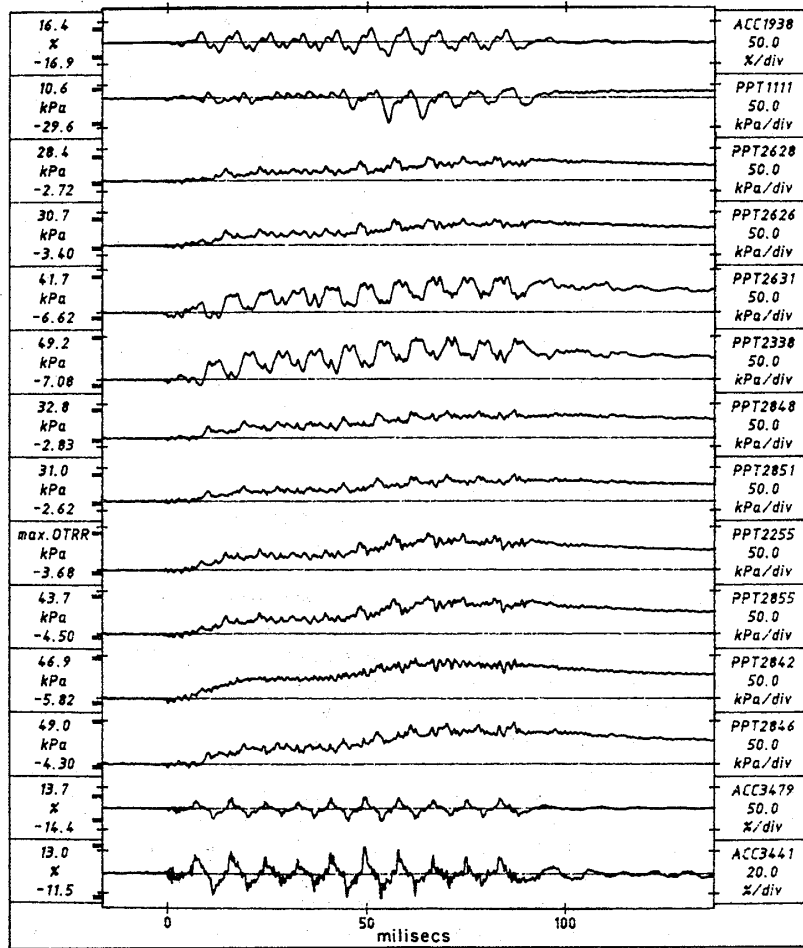


Figure 4. Complete porewater pressure data from centrifuge test.

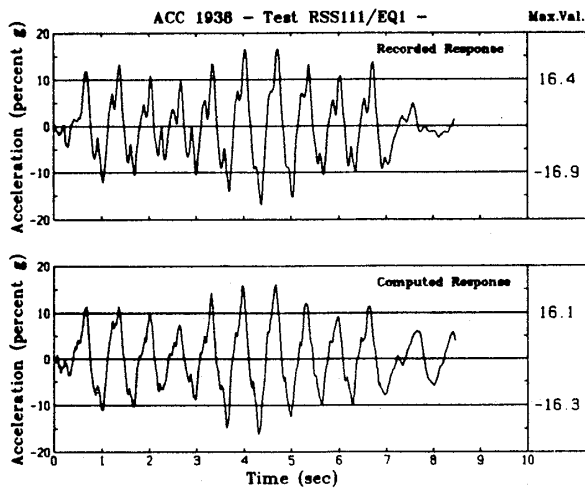


Figure 5. Recorded and computed horizontal accelerations at ACC 1938.

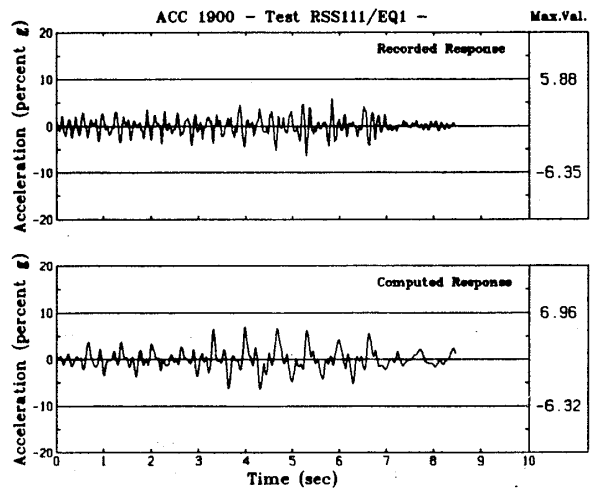


Figure 6. Recorded and computed vertical accelerations at ACC 1900.

The vertical accelerations due to rocking as recorded by ACC 1900 and those computed by TARA-3 are shown in Fig. 6. Again, the computed accelerations closely match the recorded accelerations in both peak values and frequency content. Note that the frequency content of the vertical accelerations is much higher than that of either the horizontal acceleration at the same level in the structure or that of the input motion. This occurs because the foundation soils are much stiffer under the normal compressive stresses due to rocking than under the shear stresses induced by the horizontal accelerations.

3.2 Computed and Measured Porewater Pressures

The porewater pressures in the free field recorded by PPT 2851 are shown in Fig. 7. In this case the changes in the mean normal stresses are not large and the fluctuations of the total porewater pressure about the residual value are relatively small. The peak residual porewater pressure, in the absence of drainage, is given directly by the pressure recorded after the earthquake excitation has ceased. In the present test, significant shaking ceased after 7 seconds. A fairly reliable estimate of the peak residual pressure is given by the record between 7 and 7.5 seconds. The recorded value is slightly less than the value computed by TARA-3 but the

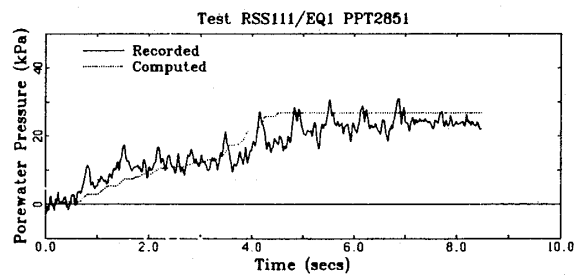


Figure 7. Recorded and computed porewater pressures at PPT 2851.

overall agreement between measured and computed pressures is quite good.

As the structure is approached, the recorded porewater pressures show the increasing influence of soil-structure interaction. The pressures recorded by PPT 2846 adjacent to the structure (Fig. 8) show somewhat larger oscillations than those recorded in the free field. This location is close enough to the structure to be affected by the cyclic normal stresses caused by rocking. The recorded peak value of the residual porewater pressure is given by the relatively flat portion of the record between 7 and 7.5 seconds. The computed and recorded values agree very closely.

Transducer PPT 2338 is located directly under the structure near the edge and was subjected to large cycles of normal stress due to rocking of the structure. These fluctuations in stress resulted in

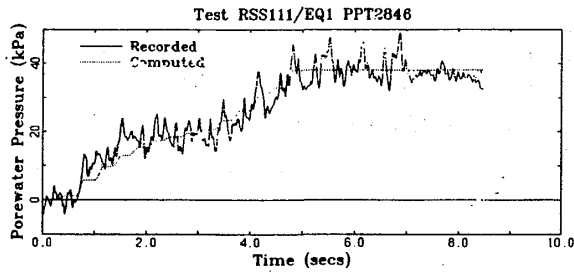


Figure 8. Recorded and computed porewater pressures at PPT 2846.

similar fluctuations in mean normal stress and hence in porewater pressure. This is clearly evident in the porewater pressure record shown in Fig. 9. The higher frequency peaks superimposed on the larger oscillations are due to dilations caused by shear strains. The peak residual porewater pressure which controls stability is observed between 7 and 7.5 seconds just after the strong shaking has ceased and before significant drainage has time to occur. The computed and measured residual porewater pressures agree very closely.

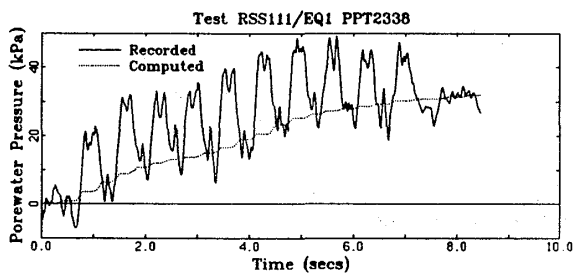


Figure 9. Recorded and computed porewater pressures at PPT 2338.

Contours of computed porewater pressures are shown in Fig. 10. They indicate very symmetrical distribution of

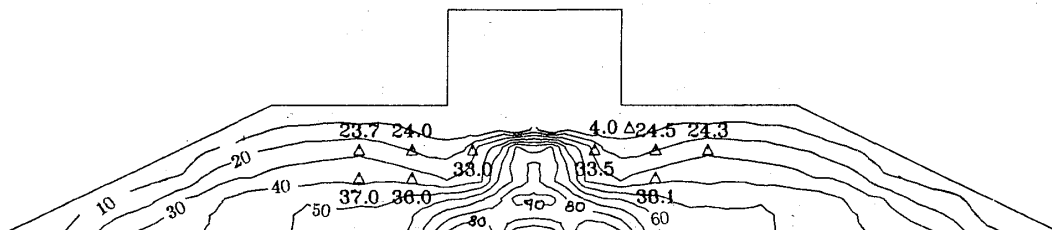


Figure 10. Contours of computed porewater pressures.

residual porewater pressure. Recorded values are also shown in this figure.

3.3 Stress-Strain Response

It is of interest to contrast the stress-strain response of the sand under the structure with that of the sand in the free field. The stress-strain response at the location of porewater pressure transducer PPT 2338 is shown in Fig. 11. Hysteretic behaviour is evident but the response for the most part is not strongly nonlinear. This is not surprising as the initial effective stresses under the structure were high and the porewater pressures reached a level of only about 20% of the initial effective vertical stress. The response in the free field at the location of PPT 2851 (Fig. 12) is strongly nonlinear with large hysteresis loops indicating considerable softening due to high porewater pressures and shear strain. At this location the porewater pressures reached about 80% of the initial effective vertical pressure.

4. ANALYSIS OF DAMS

Since the development of TARA-3 in 1986, it has been used to estimate the seismic response of a number of dams. In particular, it has been used to determine the peak dynamic displacements and the post-earthquake permanent deformations. Typical results for the proposed Lukwi tailings dam in Papua New Guinea will be presented to show the kind of data that is provided by a true nonlinear effective stress method of analysis (Finn et al., 1987). First, however, the framework of a TARA-3 analysis as applied to dams will be presented.

TARA-3 conducts both static and dynamic analysis. A static analysis is first

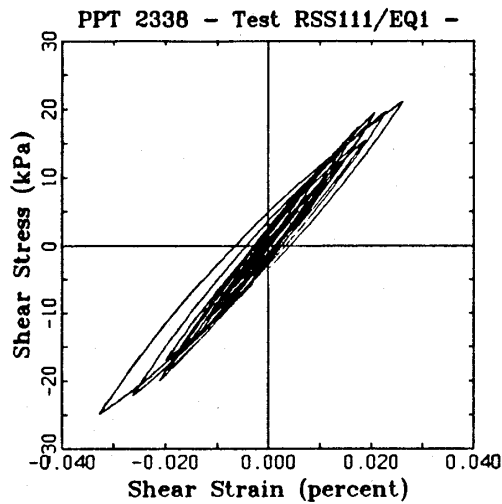


Figure 11. Stress strain response under the structure.

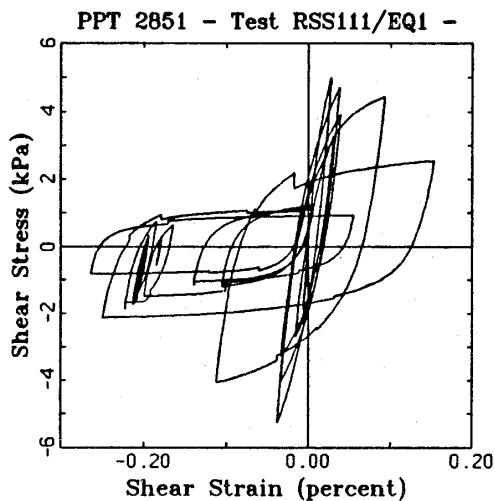


Figure 12. Stress strain response in the free field.

carried out to determine the stress and strain fields throughout the cross-section of the dam at the end of construction. The program can simulate the gradual construction of the dam.

Dynamic analysis in each element of the dam starts from the static stress-strain condition as shown in Fig. 13. This leads to accumulating permanent deformations in the direction of the smallest residual resistance to deformation. Methods of dynamic analysis commonly used in practice ignore the static strains in the dam and start from the origin of the

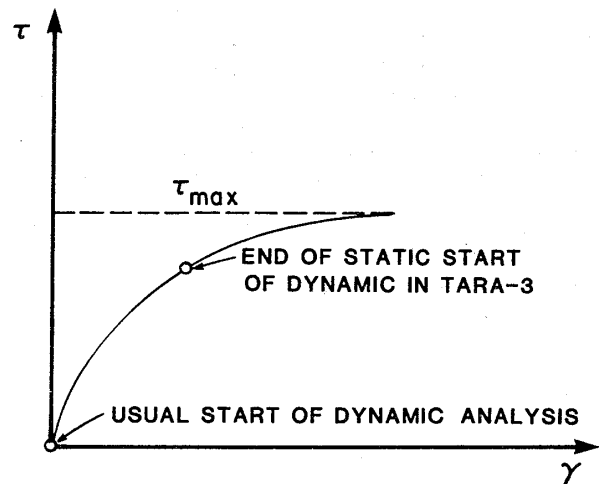


Figure 13. Different ways of initiating dynamic analysis.

stress-strain curve in all elements even in those which carry high shear stresses. TARA-3 also allows the analysis to start from the zero stress-strain condition, if it is desired to follow current practice.

As shaking proceeds, two phenomena occur; porewater pressures develop in saturated portions of the embankment and, in the unsaturated regions, volumetric strains and associated settlements develop. The program takes into account the effects of the porewater pressures on moduli and strength during dynamic analysis and estimates the additional deformations due to gravity acting on the softening soil. At the end of the earthquake, additional settlements occur due to consolidation as the seismically induced residual porewater pressures dissipate. The final deformed shape of the dam results from the sum of permanent deformations due to the hysteretic dynamic stress-strain response, constant volume deformations in saturated portions of the embankment, volumetric strains in unsaturated portions and deformations due to consolidation as the seismic porewater pressures dissipate. The final post-earthquake deformed shape of a saturated embankment computed by TARA-3 is shown in Fig. 14. This shows the classical spreading due to high porewater pressures.

The post-earthquake deformed shape of an embankment with a central core is shown in Fig. 15. The water table is about 1.7 m below the crest. Only the upstream segment to the left of the core

is saturated and generates high porewater pressure during earthquake shaking. Large deformations occur upstream and the core is strongly deformed towards the upstream side. Although the deformations in this case are contained, they are sufficient to cause severe cracking around the core.

These examples show the ability of TARA-3 to predict phenomenologically observed deformation modes in embankments during earthquakes.

4.1 Lukwi Tailings Dam

The finite element representation of the Lukwi tailings dams is shown in Fig. 16. The sloping line in the foundation is a plane between two foundation materials. Upstream to the left is a limestone with shear modulus $G = 6.4 \times 10^6$ kPa and a shear strength defined by $c' = 700$ kPa and $\phi' = 45^\circ$. The material to the right

is a siltstone with a low shearing resistance given by $c' = 0$ and $\phi' = 12^\circ$. The shear modulus is approximately $G = 2.7 \times 10^6$ kPa. The difference in strength between the foundation soils is reflected in the dam construction. The upstream slope on the limestone is steep whereas the downstream slope on the weaker foundation is much flatter and has a large berm to ensure stability.

The dam was subjected to strong shaking with a peak acceleration of 0.33 g (Fig. 17). The response of the limestone foundation is almost elastic as shown in Fig. 18 by the shear stress-shear strain response for a typical element.

The response of the siltstone foundation is strongly nonlinear. The deformations increase progressively in the direction of the initial static shear stresses as shown in Fig. 19. Since the analysis starts from the initial post-construction stress-strain condition subsequent large dynamic stress impulses

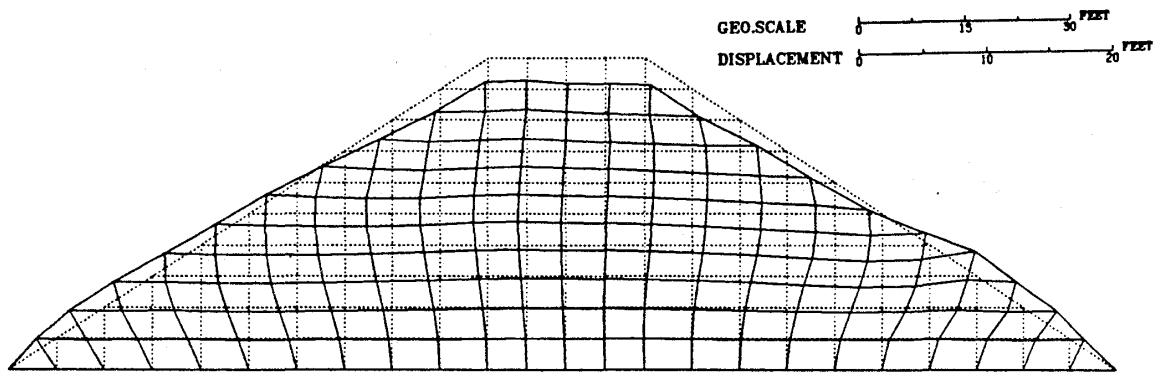


Figure 14. Deformed shape of uniform embankment after earthquake.

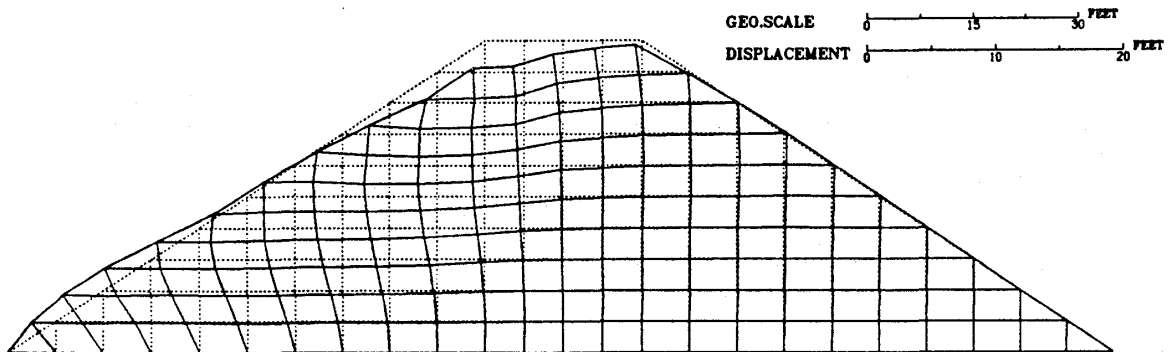


Figure 15. Deformed shape of central core embankment after earthquake.

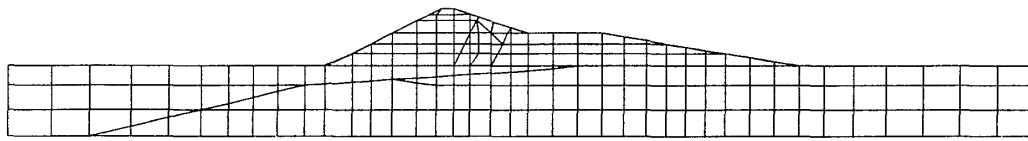


Figure 16. Finite element idealization of Lukwi tailings dam.

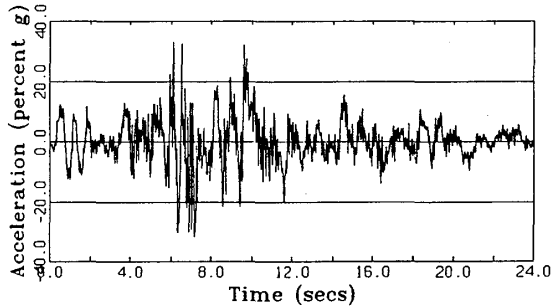


Figure 17. Input motion of analysis of Lukwi tailings dam.

move the response close to the highly nonlinear part of the stress-strain curve. It may be noted that the hysteretic stress-strain loops all reach the very flat part of the stress-strain curve, thereby ensuring successively large plastic deformations.

An element in the berm also shows strong nonlinear response with considerable hysteretic damping (Fig. 20).

The acceleration time history of a point near the crest in the steeper upstream slope is shown in Fig. 21. The displacement time history of the point is shown in Fig. 22. Note that the permanent deformation is of the order of 25 cm. Most of this was generated by a large permanent slip which occurred about 8 secs after the start of shaking.

The deformed shape of the central portion of the dam is shown to a larger scale in Fig. 23.

5. CONCLUSIONS

Phenomenological aspects of soil-structure interaction are clearly demonstrated in centrifuge tests such as high frequency rocking response, the effects of rocking on porewater pressure patterns and the distortion of free-field motions and porewater pressures by the presence of a structure.

The comparison between measured and computed responses for the centrifuge model of a structure embedded in a satur-

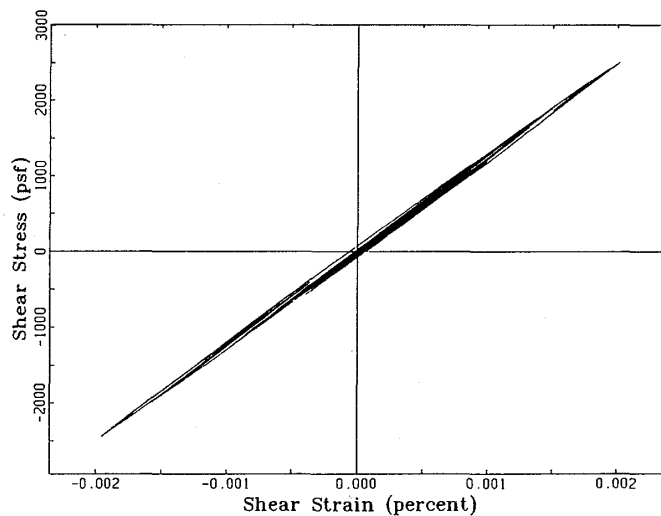


Figure 18. Shear stress-shear strain response of limestone foundation.

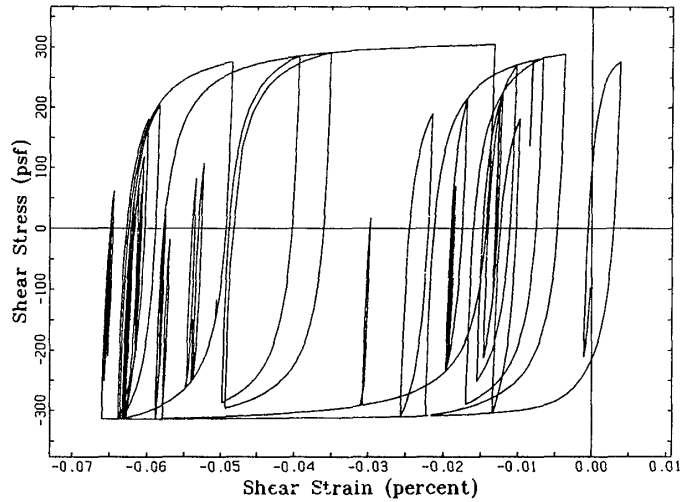


Figure 19. Shear stress-shear strain response of siltstone foundation.

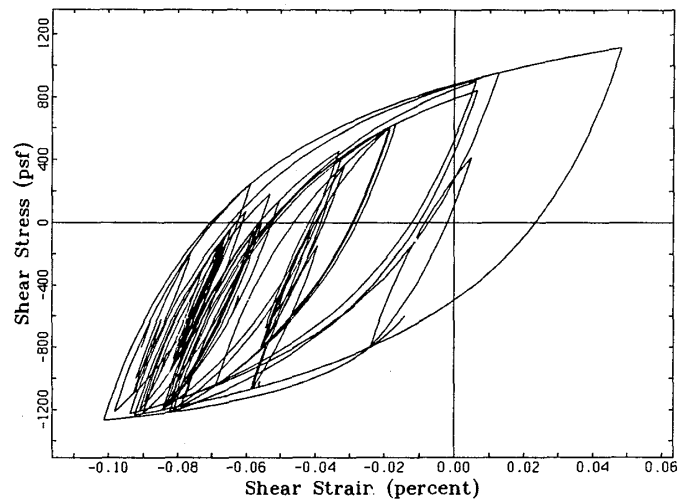


Figure 20. Shear stress-shear strain response in the berm.

ated sand foundation demonstrates the wide ranging capability of TARA-3 for performing complex effective stress soil-structure interaction analysis with acceptable accuracy for engineering purposes. Seismically induced residual porewater pressures are satisfactorily predicted even when there are significant effects of soil-structure interaction. Computed accelerations agree in magnitude, frequency content and distribution of peaks with those recorded. In particular, the program was able to model the high frequency rocking vibrations of the model structures. This is an especially difficult test of the ability of the

program to model soil-structure interaction effects.

The program TARA-3 can compute directly the permanent deformations of earth dams under seismic loading. It can reproduce the lateral spreading characteristic of loose sand embankments with high porewater pressures and the asymmetrical deformation fields of dams with impermeable cores.

The utility of TARA-3 in practice was demonstrated by the analysis of the Lukwi tailings dam. Computed stress-strain responses show the widely different responses of the different foundation materials to the design earthquake. The

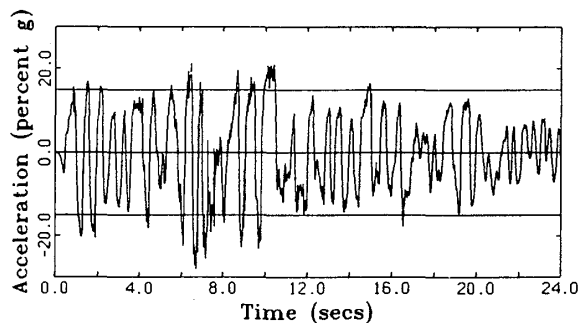


Figure 21. Computed accelerations of a point near the crest.

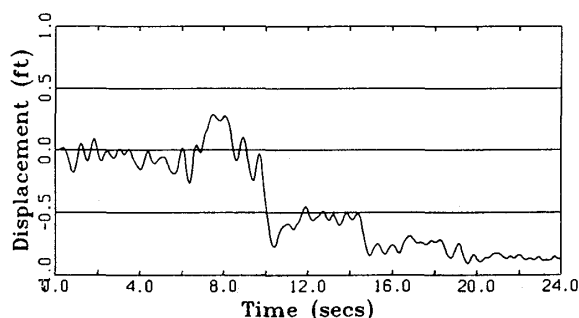


Figure 22. Displacement history of a point near the crest.

computed final deformed shape of the dam itself reflected clearly the influence of dam geometry and the different foundation materials.

The nonlinear effective stress analysis provides a very clear overall picture of the response of the dam to the design earthquake as well as providing the designer with all the details necessary in zones of potential concern.

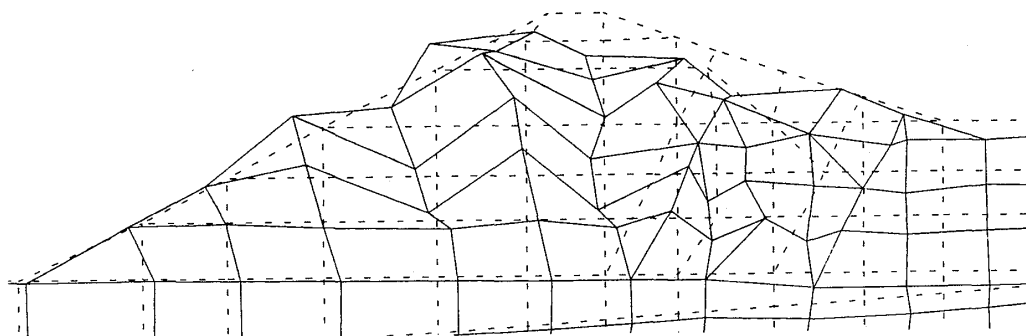


Figure 23. Deformed shape of the dam after the earthquake to enlarged scale.

6. ACKNOWLEDGEMENTS

This research was supported financially by the U.S. Government through the European Research Office of the U.S. Army and the National Science and Engineering Research Council of Canada under Grant No. 1498. The project was managed by W. Grabau and J.C. Comati of the European Research Office, U.S. Army London; R.H. Ledbetter of USAE Waterways Experiment Station, Vicksburg, Miss.; and L.L. Beratan, Office of Research, U.S. Nuclear Regulatory Commission. The centrifuge tests were conducted by R. Dean, F.H. Lee and R.S. Steedman of Cambridge University, U.K, under a separate contract. Technical assistance was provided by Chris Collinson who also operated the centrifuge. The tests were under the general direction of A.N. Schofield, Cambridge University and were monitored by the first author on behalf of USAE. Description of model test and the related figures are used by permission of Cork Geotechnics Ltd., Ireland. Data from the Lukwi tailings dam analysis are used with permission of Klohn Leonoff Consultants Ltd., Richmond, B.C., Canada.

REFERENCES

- Barton, Y.O. (1982). Laterally Loaded Model Piles in Sand; Centrifuge Tests and Finite Element Analyses, Ph.D. Thesis, Cambridge University, Engineering Department.
- Dickmen, S.U. and Ghaboussi, J. (1984). Effective Stress Analysis of Seismic Response and Liquefaction: Theory, Journal of the Geotech. Eng. Div., ASCE, Vol. 110, No. 5, Proc. Paper 18790, pp. 628-644.

- Duncan, J.M. and C.-Y. Chang. (1970). Nonlinear Analysis of Stress and Strain in Soils, *J. Soil Mech. Found. Div. ASCE*, 96 (SM5), 1629-1651.
- Finn, W.D. Liam. (1985). Dynamic Effective Stress Response of Soil Structures; Theory and Centrifugal Model Studies, *Proc. 5th Int. Conf. on Num. Methods in Geomechanics*, Nagoya, Japan, Vol. 1, 35-36.
- Finn, W.D. Liam and Bhatia, S.K. (1980). Verification of Nonlinear Effective Stress Model in Simple Shear, Application of Plasticity and Generalized Stress-Strain in Geotechnical Engineering, *ASCE, Editors, R.N. Yong and E.T. Selig*, pp. 241-252.
- Finn, W.D. Liam and S.K. Bhatia. (1981). Prediction of Seismic Porewater Pressures, *Proceedings in the Tenth Int. Conf. on Soil Mechanics and Foundation Engineering*, Vol. 3, A.A. Balkema Publishers, Rotterdam, Netherlands, pp. 201-206.
- Finn, W.D. Liam, Iai, S. and Ishihara, K. (1982). Performance of Artificial Offshore Islands Under Wave and Earthquake Loading: Field Data Analyses, *Proceedings of the 14th Annual Offshore Technology Conference*, Houston, Texas, May 3-6, Vol. 1, OTC Paper 4220, pp. 661-672.
- Finn, W.D. Liam, W.K. Lee and G.R. Martin. (1976). An Effective Stress Model for Liquefaction, *Journal of the Geotechnical Engineering Division, ASCE*, Vol. 103, No. GT6, Proc. Paper 13008, 517-533.
- Finn, W.D. Liam, Lo, R.C. and Yogendrakumar, M. (1987). Dynamic Nonlinear Analysis of Lukwi Tailings Dam, *Soil Dynamics Group, Dept. of Civil Engineering, University of British Columbia, Vancouver, B.C., Canada*.
- Finn, W.D. Liam, G.R. Martin and M.K.W. Lee. (1978). Comparison of Dynamic Analyses for Saturated Sands. *Proceedings of the ASCE Specialty Conference on Earthquake Engineering and Soil Dynamics*. Vol. I, ASCE, New York, N.Y., pp. 472-491.
- Finn, W.D. Liam, R. Siddharthan, and R.H. Ledbetter. (1985a). Soil-Structure Interaction During Earthquakes, *Proc. 11th Int. Conf. of the Int. Society of Soil Mech. and Found. Engineers*, San Francisco, California, August 11-14.
- Finn, W.D. Liam, R. Siddharthan, F. Lee and A.N. Schofield. (1984). Seismic Response of Offshore Drilling Islands in a Centrifuge Including Soil-Structure Interaction. *Proc., 16th Annual Offshore Technology Conf.*, Houston, Texas, OTC Paper 4693.
- Finn, W.D. Liam, R.S. Steedman, M. Yogendrakumar, and R.H. Ledbetter. (1985b). Seismic Response of Gravity Structures in a Centrifuge, *Proc. 17th Annual Offshore Tech. Conf.*, Houston, Texas, OTC Paper 4885, 389-394.
- Finn, W.D. Liam, M. Yogendrakumar, N. Yoshida, and H. Yoshida. (1986). TARA-3: A Program for Nonlinear Static and Dynamic Effective Stress Analysis, *Soil Dynamics Group, University of British Columbia, Vancouver, B.C.*
- Goodman, R.E., R.L. Taylor and T.L. Brekke. (1968). A Model for the Mechanics of Jointed Rock, *J. Soil Mech. and Found. Div. ASCE*, 94 (SM3), 637-659.
- Iai, S., Tsuchida, H. and Finn, W.D. Liam (1985). An Effective Stress Analysis of Liquefaction at Ishinomaki Port During the 1978 Miyagi-Ken-Oki Earthquake, *Report of the Port and Harbour Research Institute*, Vol. 24, No. 2, pp. 1-84.
- Ishihara, K. and Towhata, I. (1982). Dynamic Response of Level Ground Based on the Effective Stress Method. Ch. 7, *Soil Mechanics - Transient and Cyclic Loads*, Edited by G.N. Pande and O.C. Zienkiewicz, John Wiley and Sons Ltd., New York, N.Y., pp. 133-172.
- Lysmer, J., Udaka, T., Tsai, C.F. and Seed, H.B. 1975. FLUSH: A Computer Program for Approximate 3-D Analysis of Soil-Structure Interaction Problems. *Report No. EERC 75-30*, Earthquake Engineering Research Center, University of California, Berkeley, California.
- Martin, G.R., W.D. Liam Finn, and H.B. Seed. (1975). Fundamentals of Liquefaction Under Cyclic Loading, *Soil Mech. Series Rpt. No. 23*, Dept. of Civil Engineering, University of British Columbia, Vancouver; also *Proc. Paper 11284, J. Geotech. Eng. Div. ASCE*, 101 (GT5): 324-438.
- Masing, G. (1926). *Eigenspannungen und Verfestigung beim Messing*, *Proceedings, 2nd Int. Congress of Applied Mechanics*, Zurich, Switzerland.
- Prevost, J.H., Cuny, B., Hughes, T.J.R. and Scott, R.F. (1981). Offshore Gravity Structures: Analysis, *Journal of Geotechnical Engineering Division, ASCE*, Vol. 107, No. GT2, pp. 143-165.
- Schnabel, P.B., Lysmer, J. and Seed, H.B. (1972). SHAKE: A Computer Program for Earthquake Response Analysis of Horizontally Layered Sites, *Report No. EERC 72-12*, Earthquake Engineering

- Research Center, University of California, Berkeley, California.
- Schofield, A.N. (1981). Dynamic and Earthquake Geotechnical Centrifuge Modelling, Proceedings Int. Conf. on Recent Advances in Geot. Engineering and Soil Dynamics, St. Louis, Missouri, Vol. III: 1081-1100.
- Seed, H.B. (1979a). Considerations in the Earthquake-Resistant Design of Earth and Rockfill Dams, 19th Rankine Lecture, Geotechnique 29, No. 3, pp. 215-263.
- Seed, H.B. (1979b). Soil Liquefaction and Cyclic Mobility Evaluation for Level Ground During Earthquakes, Journal of Geotechnical Engineering Division, ASCE, Vol. 105, No. GT2, pp. 201-255.
- Seed, H.B., I.M. Idriss and I. Arango. (1983). Evaluation of Liquefaction Potential Using Field Performance Data, Journal of Geotechnical Engineering Division, Vol. 109, No. 3, pp. 458-482.
- Siddharthan, R. and W.D. Liam Finn (1982). TARA-2, Two dimensional Nonlinear Static and Dynamic Response Analysis, Soil Dynamics Group, University of British Columbia Vancouver, Canada.
- Yogendrakumar, M. and W.D. Liam Finn. (1986a).. SIMCYC2: A Program for Simulating Cyclic Simple Shear Tests on Dry or Saturated Sands, Report, Soil Dynamics Group, Dept. of Civil Engineering, University of British Columbia, Vancouver, Canada.
- Yogendrakumar, M. and W.D. Liam Finn. (1986b). C-PRO: A Program for Simulating Cyclic Simple Shear Tests on Dry and Saturated Sands, Report, Soil Dynamics Group, Dept. of Civil Engineering, University of British Columbia, Vancouver, Canada.
- Zienkiewicz, O.C., Chang, C.T. and Hinton, E. (1978). Nonlinear Seismic Response and Liquefaction, Int. J. Num. and Analytical Meth. Geomechanics, 2(4), 381-404.

